JACS
JOURNAL OF THE AMERICAN CHEMICAL SOCIETY
Communication
pubs.acs.org/JACS

Pursuit of Record Breaking Energy Barriers: A Study of Magnetic Axiality in Diamide Ligated Dy^{III} Single-Molecule Magnets

Katie L. M. Harriman,[†] Jonathan L. Brosmer,[‡] Liviu Ungur,*[,§,∥] Paula L. Diaconescu,*[,‡] and Muralee Murugesu*[,†]

[†]Department of Chemistry and Biomolecular Sciences, University of Ottawa, Ottawa, Ontatio K1N 6N5, Canada
[‡]Department of Chemistry and Biochemistry, University of California, Los Angeles, Los Angeles, California 90095, United States
[§]Theory of Nanomaterials Group and INPAC − Institute of Nanoscale Physics and Chemistry, Katholieke, Universiteit Leuven, Celestijnenlaan 200F, 3001 Leuven, Belgium
[∥]Theoretical Chemistry, Lund University, Getingevagen 60, 22100 Lund, Sweden

Supporting Information

ABSTRACT: Dy^{III} single-ion magnets (SIMs) with strong axial donors and weak equatorial ligands are attractive model systems with which to harness the maximum magnetic anisotropy of Dy^{III} ions. Utilizing a rigid ferrocene diamide ligand (NN^{TBS}), a Dy^{III} SIM, $(NN^{TBS})DyI(THF)_2$, **1-Dy** (NN^{TBS} = fc(NHS*it*BuMe$_2$)$_2$, fc = 1,1′-ferrocenediyl), composed of a near linear arrangement of donor atoms, exhibits a large energy barrier to spin reversal (770.8 K) and magnetic blocking (14 K). The effects of the transverse ligands on the magnetic and electronic structure of **1-Dy** were investigated through *ab initio* methods, eliciting significant magnetic axiality, even in the fourth Kramers doublet, thus demonstrating the potential of rigid diamide ligands in the design of new SIMs with defined magnetic axiality.

Magnetic anisotropy is arguably the most influential parameter that determines the performance of a lanthanide single-molecule magnet (SMM). The ability to design molecular species with defined magnetic axiality has allowed chemists to produce molecules with large energy barriers to spin reversal (U_{eff}) and, in some cases, magnetic blocking, reaching blocking temperatures (T_B) as high as 20 K.[1] Those SMMs containing only a single metal center, single-ion magnets (SIMs), have recently garnered significant interest in the field of molecular magnetism, as the observed magnetic properties exist in the absence of magnetic exchange interactions, meaning that the experimentally determined performance of SIMs must arise from the combination of unquenched orbital angular momentum and crystal field contributions. This allows a tailored synthetic approach, which, in recent years, has evolved to include high symmetry crystal fields,[1−4] the introduction of main group ligands,[5] and the implementation of bulky ligands to obtain low coordination numbers.[6] The common theme among all these approaches is to harness the maximum magnetic anisotropy from a lanthanide ion that results from the combination of a large magnetic moment and spin−orbit coupling. Contributions from the crystal field can significantly enhance the magnetic anisotropy of a lanthanide SIM. In this respect, recent reports have focused on generating design criteria for eliciting strictly axial anisotropy.[7,8]

The motivation for the current study resulted from our previous investigation of a series of dinuclear lanthanide SMMs.[9] This work utilized a rigid ferrocene diamide framework to support an inverse sandwich compound, exhibiting unprecedented uniaxial anisotropy, along the shortest Dy−N bond.[9] Thus, by removing the central bridging moiety, the crystal field imposed by the amide groups may enhance the SMM properties, since linearly coordinated negatively charged donor atoms may harness the maximum angular momentum of the Dy^{III} ion. This unique class of diamide ligands parallels the structural features of the diketiminates that have been popular in the fields of molecular magnetism, catalysis, and bioinorganic chemistry.[10,11] However, the ferrocene diamides are dianions as opposed to the monoanionic nature of diketiminates and have the ability to produce a wider bite angle, while still maintaining the rigidity of the backbone. The latter is an attractive feature if we wish to approach linearity and effectively mimic two-coordinate Dy^{III} compounds, which remain a synthetic challenge. Thus, these designer ligands represent a promising alternative to generating pseudoaxiality in Dy^{III} compounds. To this end, we discuss the properties of $(NN^{TBS})DyI(THF)_2$, **1-Dy** (NN^{TBS} = fc(NHS*it*BuMe$_2$)$_2$, fc = 1,1′ ferrocenediyl, Figure 1), which provides a unique approach toward Dy^{III} molecules with defined magnetic axiality.

The synthesis and structure of **1-Dy** were previously reported;[9] for clarity purposes, its structure will be discussed herein. Complex **1-Dy** crystallizes in the triclinic space group *P*-1. Each asymmetric unit contains a Dy^{III} ion coordinated to a NN^{TBS} ligand through two nitrogen atoms, producing a bite angle of 134.7(2)° (Figure 1a). The coordination sphere is completed by two molecules of THF and an iodide. The exact geometry of this five-coordinated Dy^{III} was confirmed via SHAPE analysis, producing results consistent with a trigonal bipyramidal geometry of D_{3h} symmetry (Table S1).[12] Short Dy−N distances of 2.21(2) and 2.20(6) Å are observed (Figure 1b), with only seven examples with Dy−N distances shorter or equal to 2.20 Å.[13−17] The Dy−N distances of **1-Dy** are smaller

Received: November 30, 2016
Published: January 11, 2017

DOI: 10.1021/jacs.6b12374
J. Am. Chem. Soc. 2017, 139, 1420−1423

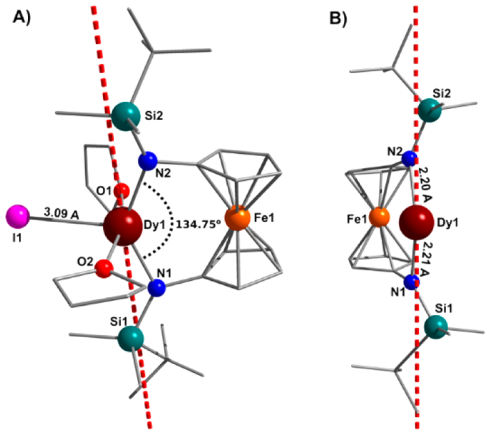

Figure 1. Structural representation of (a) **1-Dy** and (b) NN^{TBS} ligand−metal bonding. Dashed lines represent the magnetic axis in the ground, first excited, and second excited Kramers doublet (KD) states (states ±1, ±2, and ±3 in Figure 3).

than the sum of the ionic radii (2.62 Å),[18] suggesting that a dominant electrostatic interaction exists between the N atoms of the NN^{TBS} ligand and the Dy^{III} ion. The presence of such strong interactions in the axial positions of this Kramers ion has the ability to harness significant magnetic anisotropy, through taking advantage of its oblate electron density.[19] Theoretically, large T_B and U_{eff} values may be expected to arise from such a bonding interaction. Within the lattice, a minimum Dy^{III}−Dy^{III} distance of 9.776(5) Å is achieved (Figure S1). Although direct and superexchange pathways have been considered negligible at this distance, intermolecular dipolar interactions remain a possibility. At such a scale, slower relaxation processes have been attributed to dipolar mediated relaxations in 5f SIMs.[20] Collectively, the presence of strong metal−ligand interactions and the well separated nature of the paramagnetic centers are expected to yield strong slow relaxation dynamics originating from the Dy^{III} ion.

The magnetic properties of **1-Dy** were measured using a SQUID magnetometer (details are provided in the Supporting Information). Under 1000 Oe, at room temperature, the χT value of 13.99 cm^3Kmol^{-1} is in good agreement with the theoretical value of 14.17 cm^3 $Kmol^{-1}$ for a Dy^{III} ($^6H_{15/2}$, $S = 5/2$, $L = 5$, $g = 4/3$) ion (Figure S2). The obtained value is slightly smaller than the theoretical value, presumably due to splitting of the $^6H_{15/2}$ ground state.[1] Upon cooling, the χT product remains relatively constant until 8 K, revealing a well separated low-lying energy spectrum (*vide infra*). Below this temperature, the χT product rapidly drops, to a minimum at 9.67 cm^3 $Kmol^{-1}$ at 1.8 K. The abrupt decrease in the χT profile is indicative of magnetic blocking, where the system cannot reach an equilibrated population distribution. This phenomenon has been observed in other highly anisotropic SMMs.[1,6,21,22] To complement this, the isotemperature magnetization curve at 1.9 K saturates at 5.28 μ_B mol^{-1}, further suggesting the well separated nature of the ground state (Figure S3). Large separations between the ground state and excited states are highly sought after as it remains the origin for large spin reversal barriers. This finding is also in accordance with the *ab initio* determined energy of the second Kramers doublet (KD), possessing an energy of 414.6 cm^{-1} (*vide infra*). This is one of the largest separations observed between the ground state and excited states in any Dy^{III} SMMs.[1,6,21,22] This large separation ensures that thermal relaxation will at least occur via this energy, yielding an impressive barrier to the slow relaxation of the magnetization.

The presence of magnetic blocking, was probed with magnetic hysteresis measurements in the range of 50 to −50 kOe, at an average sweep rate of 23 Oe s^{-1} (Figure S4). At 1.9 K, **1-Dy** displays clear magnetic hysteresis. Upon raising the temperature, openings at $H = 0$ Oe are observed until 5 K, and at $H \neq 0$ Oe openings can be observed up to 14 K at higher magnetic fields. Comparatively, the abrupt drop in the χT product at 8 K also serves as a reference in terms of magnetic blocking. However, the discrepancy between these observed values may result as a consequence of mixed relaxation processes, specifically Raman and direct relaxations that occur at low temperature.[6] The possibility of mixed relaxation mechanisms cannot be discarded given the low temperature data of the alternating current (ac) susceptibility (Figure 2), as well as the obtained distribution of relaxation times (Tables S2 and S3).

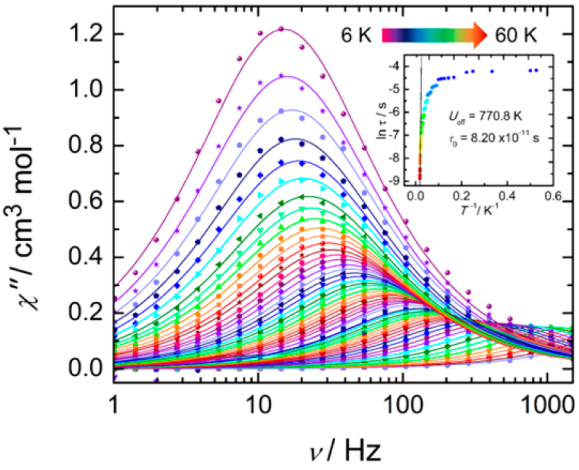

Figure 2. Frequency dependence of the χ'' magnetic susceptibility for **1-Dy** under zero applied dc field from 6 to 60 K. Solid lines represent best fits to the generalized Debye model. Inset: Relaxation time of the magnetization, $\ln(\tau)$ vs T^{-1}; the solid black line represents the linear fit to the Arrhenius equation.

Ac susceptibility measurements were completed under zero applied dc field, within the range 0.1−1500 Hz. A single peak in the out-of-phase (χ'') susceptibility was observed between 1.9 and 60 K, with shifting peak maxima toward lower frequency (Figure 2 and S5). The relaxation time (τ) was extracted for each isotemperature curve of the in-phase (χ') and χ'' susceptibilities via the generalized Debye model.[23] A narrow distribution of relaxation times was found, yielding α parameters ≤ 0.17 (Tables S2 and S3). Comparatively, fitting the Argand plots (Figure S6) to the generalized Debye model produced similar results ($\alpha \leq 0.22$), with only a single deviation occurring for the 6 K curve ($\alpha = 0.50$).

The χ'' data was fit to the Arrhenius law ($\tau = \tau_0 \exp[U_{eff}/(k_BT)]$) to give U_{eff} = 770.8 K (535.7 cm^{-1}) and $\tau_0 = 8.20 \times 10^{-11}$ s. A U_{eff} of this magnitude is rare in lanthanide based systems, as they often exhibit significant ground state tunneling arising from their classically dense energy spectra.[24] As such, there are only a few compounds that belong to this family of high U_{eff} (>700 K) SIMs.[4,6,21,25] In the case of **1-Dy**, the U_{eff} of 770.8 K is in good agreement with the calculated thermally activated relaxation through the third and fourth KDs (Figure 3). The plot of $\ln(\tau)$ vs T^{-1} remains linear

DOI: 10.1021/jacs.6b12374
J. Am. Chem. Soc. 2017, 139, 1420−1423

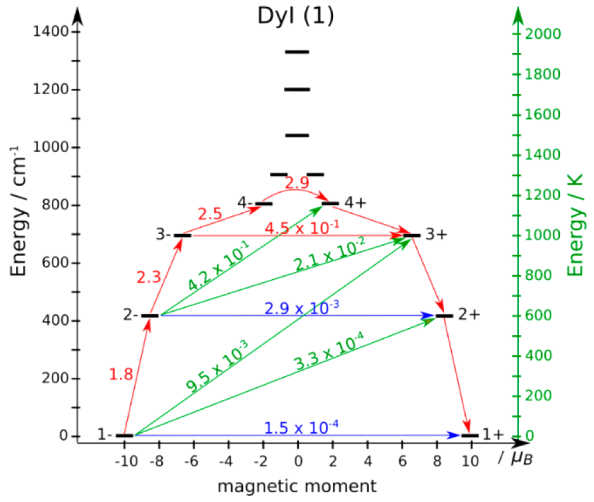

Figure 3. Magnetization blocking barrier of **1-Dy**. Arrows depict the most probable path for magnetic relaxation (red), QTM (blue) and Orbach relaxation (green). At temperatures where $\ln(\tau) = f\left(\frac{1}{T}\right)$ dependence is linear (see Figure 2, inset), the temperature assisted tunneling via KD4 is dominant. Temperature dependence of the ratio between relaxation rates in different excited states is given in SI (Figures S14 and 15 and the corresponding explanation).

in the high temperature regime (Figure 2 inset), strongly correlating to a dominant thermally activated Orbach relaxation regime.[26] The plot remains linear until 26 K, when it experiences a deviation from the Arrhenius law. The observed behavior may arise from mixed relaxation mechanisms, although it is likely dominated by quantum tunneling of the magnetization (QTM).

To probe any contribution of QTM to the obtained U_{eff}, ac measurements were completed at various static fields (0−1200 Oe) (Figure S7). The plot of χ'' vs ac frequency yielded a two peak-profile. At 100 Oe, a shoulder at low frequencies becomes evident, and is augmented by increased static fields until 400 Oe, where no signal was observed. This has similarly been observed at small fields in other Dy^{III} SIMs.[27] The Argand plots were fit via the generalized Debye model (Figure S8), providing a distribution of field dependent relaxation times with $0.89 \geq \alpha \geq 0.25$ (Table S5). To determine the origin of the secondary process, ac measurements were completed under an optimal dc field of 150 Oe. Within the range 1.9−54 K, a frequency dependent ac signal was observed (Figures S9 and S10). Below 16 K, there is minimal shifting of the χ'' peaks, as well as the introduction of the second process. Fitting the data to the Arrhenius laws yields a U_{eff} = 348.9 K (242.5 cm^{-1}) and $\tau_0 = 3.27 \times 10^{-7}$ s (Figure S11). Fitting this process revealed a distribution of relaxation times to give $0.011 \leq \alpha \leq 0.404$ (Figure S12, Table S6). From these observations, it is clear that application of static fields diminishes the SMM behavior of **1-Dy**.

Ab initio calculations were performed in order to gain additional insight into the magnetic properties and to analyze the factors that govern the magnetization blocking barrier, details are provided in the Supporting Information. The magnetization blocking barrier for **1-Dy** was calculated using a previously established methodology (Figure 3).[28,29] A small transverse magnetic moment of 1.5×10^{-4} μ_B in the ground state results in reduced QTM, leading to the zero-field SMM behavior. Similarly, tunneling through thermally activated $m_j = \pm 13/2$ is also minimized, this is due to the colinearity of the anisotropic axes of the first and second KDs (Figure 1). These findings correlate with the obtained *g*-tensors (Table S8), demonstrating significant magnetic axiality even at the $m_j = \pm 11/2$ states. Given the transverse magnetic moments (indicated above the arrows in Figure 3), the most probable pathway for magnetic relaxation encompasses the third and fourth KDs, while the U_{eff} lies only marginally below the third KD. Thus, the presence of mixed relaxation mechanisms may contribute to the lowering of U_{eff} from the anticipated energy of the third KD. Notably, the magnetic moment of an Orbach relaxation from $m_j = -13/2$ to $m_j = +9/2$ is only narrowly smaller than the tunneling between $m_j = \pm 11/2$ states (4.2×10^{-1} μ_B vs 4.5×10^{-1} μ_B), suggesting that a competition between these two pathways may also contribute to the lowering of the experimental barrier.

It is important to mention that *ab initio* results are not based on direct fitting of the experimental data (compared to various phenomenological models).[30] The methods may be applied for the investigation of molecules prior to their synthesis for the evaluation of molecular properties. In this respect, we have developed and analyzed three different models in addition to **1-Dy**, in order to see the effects of THF and iodide ligands on the magnetic properties of the title molecule. Models have been prepared from sequential removal of ligands and their respective formal charges, producing three chemically sensible models: **1-noTHF**, containing no THF ligands; **1-noI**, containing no iodide ligand; **1-noTHFnoI**, where THF and iodide ligands were removed from the molecular structure. These models allow for a direct study of the ligand field effects that originate in **1-Dy**. In understanding the factors that contribute to lowering the U_{eff}, we can then find improved ways for augmenting the local magnetic axiality in other low coordinate Dy^{III} systems. The energy splitting of the ground free ion $J = 15/2$ was obtained for all models and the title compound (Table S9). Analysis of the low-lying energy spectra reveals a strong increase in the splitting of the ground free ion in **1-noTHF**, as well as in **1-noI**. With respect to the second KD, there is a 15.8% and 15.1% increase in the energy splitting for **1-noTHF** and **1-noI**, respectively. Although the difference between **1-noTHF** and **1-noI** is minimal, in the third KD, the effect of the THF molecules are greater. Removal of such moieties produces a 22.2% increase over **1-Dy**, whereas removal of the iodide ligand only produces a 13.7% increase. This is conceivable as Dy−I bonds are characteristically weak, meaning that their contribution to the total ligand field of **1-Dy** is less relative to the oxophilic interaction of Dy^{III} with THF. It is suspected that the THF molecules are producing a competitive ligand field, perpendicular to that generated by the N atoms of NN^{TBS}, which likely contributes to the diminished U_{eff}.

In the absence of transverse ligands, **1-noTHFnoI**, a 33.3% increase in the energy splitting of the first KD is observed, with $g_Z \gg g_X, g_Y$, even in the fourth KD. This produces a near 3-fold improvement (535.7 vs 1591.1 cm^{-1}) on the U_{eff}. The obtained *g*-tensors for **1-noI** in the fourth KD are less axial in comparison to **1-Dy**, whereas **1-noTHF** and **1-Dy** display similar *g*-tensors. The inferior axiality of **1-noI** can be reasoned once again by the ligand field generated by the remaining THF, thus demonstrating the immediate significance of removing or replacing these moieties with weaker-field ligands. Through this systematic study of *g*-tensors combined with the low-lying energy spectra, we are finding ways to improve the local

DOI: 10.1021/jacs.6b12374
J. Am. Chem. Soc. 2017, 139, 1420−1423

magnetic axiality of molecular species. Future work should be devoted to finding suitable equatorial ligands that do not affect the crystal field splitting of the lanthanide ion or to avoid equatorial ligands, if possible.[6,8]

Our study highlights a new design approach toward mimicking the elusive two coordinate Dy^{III}, although the presence of coordinated solvent and an iodide ligand prevent the maximum U_{eff} that could theoretically be achieved for such a system (≈1600 cm^{-1}). The functionalized ferrocene backbone of NN^{TBS} offers a unique synthetic approach toward harnessing single-ion anisotropy. Through careful synthetic modifications, the contributions of the equatorial/transverse ligands may be altered by replacement with weaker crystal field ligands, effectively allowing for fine-tuning of the magnetic axiality. Although two coordinate Dy^{III} compounds will undoubtedly remain a synthetic challenge, the use of rigid diamide ligands represents a promising approach for imposing pseudoaxial ligand fields in the development of high temperature lanthanide based SIMs with predictable and defined magnetic axiality.

■ ASSOCIATED CONTENT

Supporting Information

The Supporting Information is available free of charge on the ACS Publications website at DOI: 10.1021/jacs.6b12374.

Experimental and computational details (PDF)

■ AUTHOR INFORMATION

Corresponding Authors

*m.murugesu@uottawa.ca (M.M.)
*liviu.ungur@chem.kuleuven.be (L.U.)
*pld@chem.ucla.edu (P.L.D.)

ORCID

Paula L. Diaconescu: 0000-0003-2732-4155
Muralee Murugesu: 0000-0002-5123-374X

Notes

The authors declare no competing financial interest.

■ ACKNOWLEDGMENTS

The authors gratefully acknowledge the University of Ottawa, CFI and NSERC grants for their financial support. The synthetic work was supported by the NSF (Grant 1362999 to P.L.D.). L.U. is a postdoc of the FWO (Fonds Wetenchappelijk Onderzoek – Vlaanderen) and also gratefully acknowledges financial support from Methusalem and INPAC grants from the K. U. Leuven.

■ REFERENCES

(1) Chen, Y.-C.; Liu, J.-L.; Ungur, L.; Liu, J.; Li, Q.-W.; Wang, L.-F.; Ni, Z.-P.; Chibotaru, L. F.; Chen, X.-M.; Tong, M.-L. *J. Am. Chem. Soc.* **2016**, *138*, 2829−2837.
(2) Meihaus, K. R.; Long, J. R. *J. Am. Chem. Soc.* **2013**, *135*, 17952−17957.
(3) Ungur, L.; Le Roy, J. J.; Korobkov, I.; Murugesu, M.; Chibotaru, L. F. *Angew. Chem., Int. Ed.* **2014**, *53*, 4413−4417.
(4) Ding, Y.-S.; Chilton, N. F.; Winpenny, R. E. P.; Zheng, Y.-Z. *Angew. Chem., Int. Ed.* **2016**, *55*, 16071−16074.
(5) Pugh, T.; Tuna, F.; Ungur, L.; Collison, D.; McInnes, E. J. L.; Chibotaru, L. F.; Layfield, R. A. *Nat. Commun.* **2015**, *6*, 7492.
(6) Gregson, M.; Chilton, N. F.; Ariciu, A.-M.; Tuna, F.; Crowe, I. F.; Lewis, W.; Blake, A. J.; Collison, D.; McInnes, E. J. L.; Winpenny, R. E. P.; Liddle, S. T. *Chem. Sci.* **2016**, *7*, 155−165.
(7) Chilton, N. F. *Inorg. Chem.* **2015**, *54*, 2097−2099.
(8) Ungur, L.; Chibotaru, L. F. *Inorg. Chem.* **2016**, *55*, 10043−10056.
(9) Huang, W.; Le Roy, J. J.; Khan, S. I.; Ungur, L.; Murugesu, M.; Diaconescu, P. L. *Inorg. Chem.* **2015**, *54*, 2374−2382.
(10) Fortier, S.; Le Roy, J. J.; Chen, C.-H.; Vieru, V.; Murugesu, M.; Chibotaru, L. F.; Mindiola, D. J.; Caulton, K. G. *J. Am. Chem. Soc.* **2013**, *135*, 14670−14678.
(11) Guillet, G. L.; Sloane, F. T.; Ermert, D. M.; Calkins, M. W.; Peprah, M. K.; Knowles, E. S.; Cizmar, E.; Abboud, K. A.; Meisel, M. W.; Murray, L. J. *Chem. Commun.* **2013**, *49*, 6635−6637.
(12) Alvarez, S.; Llunell, M. *J. Chem. Soc., Dalton Trans.* **2000**, 3288−3303.
(13) Zhang, J.; Yi, W.; Chen, Z.; Zhou, X. *Dalton Trans.* **2013**, *42*, 5826−5831.
(14) Anfang, S.; Harms, K.; Weller, F.; Borgmeier, O.; Lueken, H.; Schilder, H.; Dehnicke, K. *Z. Anorg. Allg. Chem.* **1998**, *624*, 159−166.
(15) Yang, S.; Troyanov, S. I.; Popov, A. A.; Krause, M.; Dunsch, L. *J. Am. Chem. Soc.* **2006**, *128*, 16733−16739.
(16) Zhang, P.; Zhang, L.; Wang, C.; Xue, S. F.; Lin, S. Y.; Tang, J. K. *J. Am. Chem. Soc.* **2014**, *136*, 4484−4487.
(17) Zhao, L.; Xue, S.; Tang, J. *Inorg. Chem.* **2012**, *51*, 5994−5996.
(18) Shannon, R. D. *Acta Crystallogr., Sect. A: Cryst. Phys., Diffr., Theor. Gen. Crystallogr.* **1976**, *32*, 751−767.
(19) Rinehart, J. D.; Long, J. R. *Chem. Sci.* **2011**, *2*, 2078−2085.
(20) Rinehart, J. D.; Meihaus, K. R.; Long, J. R. *J. Am. Chem. Soc.* **2010**, *132*, 7572−7573.
(21) Liu, J.; Chen, Y.-C.; Liu, J.-L.; Vieru, V.; Ungur, L.; Jia, J.-H.; Chibotaru, L. F.; Lan, Y.; Wernsdorfer, W.; Gao, S.; Chen, X.-M.; Tong, M.-L. *J. Am. Chem. Soc.* **2016**, *138*, 5441−5450.
(22) Pugh, T.; Chilton, N. F.; Layfield, R. A. *Angew. Chem., Int. Ed.* **2016**, *55*, 11082.
(23) Gatteschi, D.; Sessoli, R.; Villian, J. *Molecular Nanomagnets*. Oxford University Press: Oxford, 2006.
(24) Liddle, S. T.; van Slageren, J. *Chem. Soc. Rev.* **2015**, *44*, 6655−6669.
(25) Gupta, S. K.; Rajeshkumar, T.; Rajaraman, G.; Murugavel, R. *Chem. Sci.* **2016**, *7*, 5181−5191.
(26) Orbach, R. *Proc. R. Soc. London, Ser. A* **1961**, *264*, 458−484.
(27) Williams, U. J.; Mahoney, B. D.; DeGregorio, P. T.; Carroll, P. J.; Nakamaru-Ogiso, E.; Kikkawa, J. M.; Schelter, E. J. *Chem. Commun.* **2012**, *48*, 5593−5595.
(28) Ungur, L.; Chibotaru, L. F. *Phys. Chem. Chem. Phys.* **2011**, *13*, 20086−20090.
(29) Ungur, L.; Thewissen, M.; Costes, J.-P.; Wernsdorfer, W.; Chibotaru, L. F. *Inorg. Chem.* **2013**, *52*, 6328−6337.
(30) Ungur, L.; Chibotaru, L. F. *Chem. - Eur. J.* **2016**, DOI: 10.1002/chem.201605102.

DOI: 10.1021/jacs.6b12374
J. Am. Chem. Soc. 2017, 139, 1420−1423